Solar Energy Materials & Solar Cells 93 (2009) 1263–1267

Contents lists available at ScienceDirect

Solar Energy Materials & Solar Cells

journal homepage: www.elsevier.com/locate/solmat

Effect of P3HT:PCBM concentration in solvent on performances of organic solar cells

Woon-Hyuk Baek [a], Hyun Yang [a], Tae-Sik Yoon [a], C.J. Kang [a,b], Hyun Ho Lee [c], Yong-Sang Kim [a,d,*]

[a] Department of Nano Science and Engineering, Myongji University, Gyeonggi 449-728, Republic of Korea
[b] Department of Physics, Myongji University, Gyeonggi 449-728, Republic of Korea
[c] Department of Chemical Engineering, Myongji University, Gyeonggi 449-728, Republic of Korea
[d] Department of Electrical Engineering, Myongji University, Gyeonggi 449-728, Republic of Korea

ARTICLE INFO

Article history:
Received 31 August 2008
Received in revised form
22 January 2009
Accepted 26 January 2009
Available online 6 March 2009

Keywords:
Crystallinity
Morphology
Phase separation
Absorption
Organic solar cells

ABSTRACT

Focused on phase separation and morphologies of poly(3-hexylthiophene):[6,6]-phenyl C_{61} butyric acid methyl ester (P3HT:PCBM) active layers, we studied the effect of preparation conditions of the active layer on photovoltaic performance by changing concentration of P3HT:PCBM in the solvent. The performances of the cells varied depending on concentration of P3HT:PCBM (1:1 ratio by weight) in solvent even with the same thickness. The P3HT:PCBM active layer is prepared in cell structure of ITO/PEDOT/P3HT:PCBM/Al by changing spin-coating speed with different concentrations (1, 2 and 3 wt%) in chlorobenzene. Here, it was found that both the P3HT:PCBM concentrations and spin-coating conditions affected the crystalline structure formation, interchain interaction, morphology and phase separation during drying process of solvent and subsequent annealing.

1. Introduction

The bulk heterojunction (BHJ) solar cells have been very attractive research topic because of the advantages of the so-called plastic solar cells, which include low fabrication cost, lightness, simple fabrication process and flexibility. Because of these practical device advantages, studies have focused on stability [1–7], large area processing [8–12], indium tin oxide (ITO) free transparent electrodes [13–16], etc. [17–22]. Although their photovoltaic (PV) performances were very poor in the early stage, recent studies have reported remarkably improved PV performances of the BHJ solar cells up to 5% in single device structure through studies of annealing time, temperature and electrical treatment [23–26], molecular weight of electron donor material poly(3-hexylthiophene) (P3HT) [27,28], ratio of electron donor (P3HT), acceptor [6,6]-phenyl C_{61} butyric acid methyl ester (PCBM) [29,30] and adhesive layer on or under anode or cathode layer [31]. Especially, as annealing is indispensable for complete drying of solvent, phase separation for the BHJ formation, evolution of the film morphology and device efficiency have been investigated at different temperatures. An optimal PV performance could be obtained through de-mixing of P3HT and PCBM constitution and self-organization of BHJ materials, though the details of the annealing effects are not clearly elucidated yet. In organic thin film transistor (OTFT), chloroform and toluene are widely used solvents to dissolve P3HT [32,33]. Chlorobenzene is the most favored one in BHJ solar cells due to better solubility for PCBM and crystal packing structure [25,34]. In the several reports concerning solvent, and authors of [34–36] reported that the different morphology of active layer is determined by solubility and phase segregation process. Recently, Yang and coworkers [37–39] reported 'solvent annealing effect' related to the boiling point of the solvent, solvent drying time after spin coating and growth rate of active layer. With 'slow growth', for example, the close-packed crystalline structure and strong interchain interactions of P3HT could be obtained using high boiling point solvent and large enough solvent evaporation time. In this study, we investigated the effect of P3HT:PCBM concentration in the solvent during the active solution preparation in chlorobenzene, which is expected to alter the crystalline structure of P3HT:PCBM and its PV performances.

2. Experimental

Regioregular P3HT (Rieke Metals, inc.) and PCBM (Sigma-Aldrich) were used as active layers without any further purification. The P3HT and PCBM (1:1 weight ratio) were dissolved in

* Corresponding author at: Department of Nano Science and Engineering, Myongji University, Gyeonggi 449-728, Republic of Korea. Tel.: +81 31 338 6327; fax: +81 31 321 0271.
E-mail address: kys@mju.ac.kr (Y.-S. Kim).

0927-0248/$ - see front matter © 2009 Elsevier B.V. All rights reserved.
doi:10.1016/j.solmat.2009.01.019

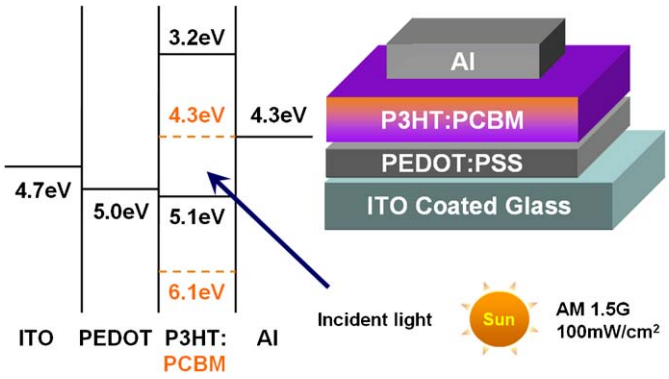

Fig. 1. Schematic diagram of the BHJ solar cell and its energy band structure.

chlorobenzene to make 1, 2 and 3 weight percent (wt%) solutions and stirred at 60 °C for 1 h. Poly(3,4-ethylenedioxythiophene:poly(styrene sulfonate) (PEDOT:PSS; Baytron P HC V4), de-ionized (DI) water and dimethyl sulphoxide (DMSO) were used as anodic buffer layers and stirred for one day at room temperature. DI water and DMSO were added to reduce the viscosity and enhance conductivity, respectively. By adding DI water, series resistance of the solar cell was reduced with decrease in buffer-layer thickness although the conductivity of solution reduced. The ITO (15 Ω/square) coated glass substrate was cleaned in ultrasonic bath with DI water, acetone and isopropyl alcohol for 15 min and then cleaned with UV-ozone for 30 min. The stirred anodic buffer solution PEDOT was spin coated at 5000 rpm for 60 s and baked at 150 °C for 10 min. Photoactive layer (P3HT:PCBM) solution was spin coated at 300 rpm (1 wt%), 1000 rpm (2 wt%) and 3000 rpm (3 wt%) for 60 s to form 100 (±5)-nm-thick film. Its thickness was measured using surface profiler (alpha-step 500). Al (100 nm) cathode was thermally evaporated through shadow mask defining active area of 0.1 cm^2. Thermal annealing process was conducted at 150 °C in thermal oven for 10 min under N_2 ambient. The annealing in oven provides accurate and isothermal annealing condition within the sample than annealing on hot plate. The entire fabrication process was conducted in air environment except for thermal annealing. Fig. 1 shows schematic diagram of the BHJ solar cell and its energy band structure. The current density versus voltage characteristics were measured with *J–V* curve tracer (Eko MP-160) with solar simulator (Yamashita denso) under AM 1.5 G (100 mW/cm^2) irradiation intensity. UV/visible spectrophotometer (Shimadzu UV-1601) was used to study absorption spectra of the P3HT:PCBM films on PEDOT-coated ITO glass substrates. The crystalline structure of the active layer was analyzed using two-dimensional Grazing Incidence X-ray Diffraction (2D GIXRD; Bruker AXS with an X-ray wavelength of 1.54056 Å). Surface morphology and phase separation of the active layer were measured using atomic force microscope (AFM; XE-100, Park Systems) in tapping mode and field-emission transmission electron microscope (FE-TEM; JEM-2100F, JEOL). For TEM analysis, specimens are prepared by floating the active layers onto the DI water, followed by picking them up with Cu grid.

3. Results and discussion

Fig. 2 shows UV/visible absorption spectra of as-casted and annealed P3HT:PCBM at 150 °C for 10 min prepared from different concentrations in the solvent. As concentrations of as-casted P3HT:PCBM film decreases, absorption peak of P3HT (~500 nm) gradually increases and broadens, besides showing red-shift. This tendency depends on concentration and this is clear after thermal annealing. It demonstrates that thermal annealing and

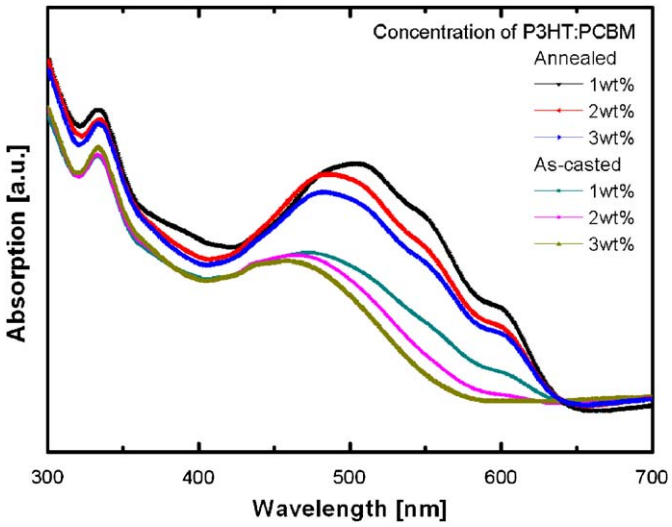

Fig. 2. UV/visible absorption spectra of as-casted and annealed (at 150 °C for 10 min) films with different concentrations of P3HT:PCBM.

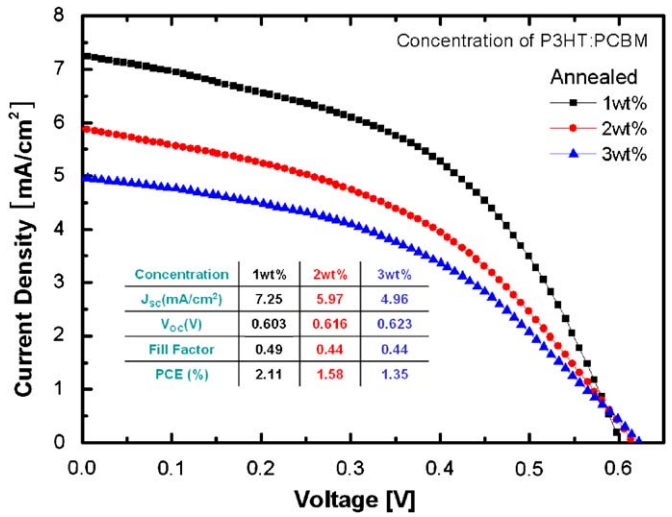

Fig. 3. Current density–voltage characteristics of BHJ solar cells with different concentrations of P3HT:PCBM at an irradiation intensity of 100 mW/cm^2.

preparation of P3HT:PCBM film with lowered concentration, as corresponding to slower evaporation of solvent, result in the higher degree of crystallinity and longer conjugation length [40–42] of P3HT. The shift of π–π* transition absorption peaks to higher energy indicates an increasing density of conformational defects, equivalent to non-plarnarity, and causes loss of conjugation [41,42]. Especially, the as-casted 1 wt% film with the lowest coating speed shows similar absorption intensity with annealed films of 2 and 3 wt% films. It is believed that a slow evaporation of solvent which is beneficial for photo-absorption of P3HT:PCBM layer leads to strong interchain interaction before solvent is completely evaporated [39,43,44]. On the other side, PCBM peak (~330 nm) shows almost the same intensity irrespective of the concentrations of P3HT:PCBM, although intensity is slightly increased by annealing. It indicates that interactions of PCBM molecules are less dependent on evaporation time of solvent or annealing, than P3HT.

Current density–voltage (*J–V*) characteristic results are in accordance with the absorption spectra as shown in Fig. 3. The performances of as-casted devices were very poor and did not

show diode characteristics except for 1 wt% of P3HT:PCBM device (not shown here). However, the performances of solar cells were considerably improved after annealing. With 1 wt% of P3HT:PCBM device, the highest short-circuit current density (J_{sc}) could be obtained (7.25 mA/cm^2). The J_{sc} was dramatically decreased by increasing P3HT:PCBM concentration, i.e., 5.96 mA/cm^2 for 2 wt% and 4.97 mA/cm^2 for 3 wt%. It is concluded that the decreased J_{sc} was due to the reduced degree of P3HT crystallinity as shown in the absorption intensity of the active layer and GIXRD data (discussed in Fig. 6). The fill factor (FF) of 1 wt% device was calculated to be 49%, whereas it was 44% for 2 and 3 wt% devices. Though these values are lower than the previously reported ones [25,31], this observation shows the clear tendency of PV performances to depend on concentration. It is expected that FF and efficiency can be improved by fabricating the solar cells under inert gas condition [35]. Open circuit voltage (V_{oc}) was slightly decreased by the decrease in P3HT:PCBM concentration. Typically, V_{oc} is governed by the energetic relationship between the donor and the acceptor. Specifically, the energy difference between the highest occupied molecular orbital (HOMO) of the donor and the lowest unoccupied molecular orbital (LUMO) of the acceptor is closely correlated to the V_{oc} value [21]. HOMO and LUMO splitting of the polymer converge toward the analogous value which corresponds to the reduction of effective bandgap as the interchain interaction and the chain length are increased [45]. Therefore, it can be explained that results of the reduced V_{oc} originated from reduced effective bandgap compared to relative difference between HOMO and LUMO of P3HT [39,45]. As shown in Fig. 2 of UV/visible spectroscopy, the strong interchain interaction was also observed by slow evaporation of the solvent with low concentration of P3HT:PCBM. Therefore, V_{oc} of the device with 1 wt% of P3HT:PCBM was slightly decreased.

In AFM topographic images of P3HT:PCBM layers, as shown in Fig. 4 (a; 1 wt%, b; 2 wt%, c; 3 wt%), peak to valley height and rms roughness gradually increased as concentration of P3HT:PCBM increased. Peak to valley heights were 4.6, 6.6 and 7.4 nm and rms roughnesses were 0.58, 0.69 and 1.02 nm for 1, 2 and 3 wt% of P3HT:PCBM, films, respectively. In the previously reported studies about morphology [38], rough surface was mentioned as the self-organization signature of polymer. In our case, however, surface roughness is not correlated to phase separation because phase images show very fine feature of phase separation than the roughened image of the film. The phase images shown in Fig. 4 (d; 1 wt%, e; 2 wt%, f; 3 wt%) reveal that the interpenetrating networks and uniform distributions of P3HT:PCBM profitable for charge generation and transportation are clear in Fig. 4(d) for 1 wt% device than for 2 and 3 wt% devices.

To study the details of phase separation and ordering of active layer, FE-TEM analysis was investigated as shown in Fig. 5. With all specimens, nanoscale interpenetrating networks of

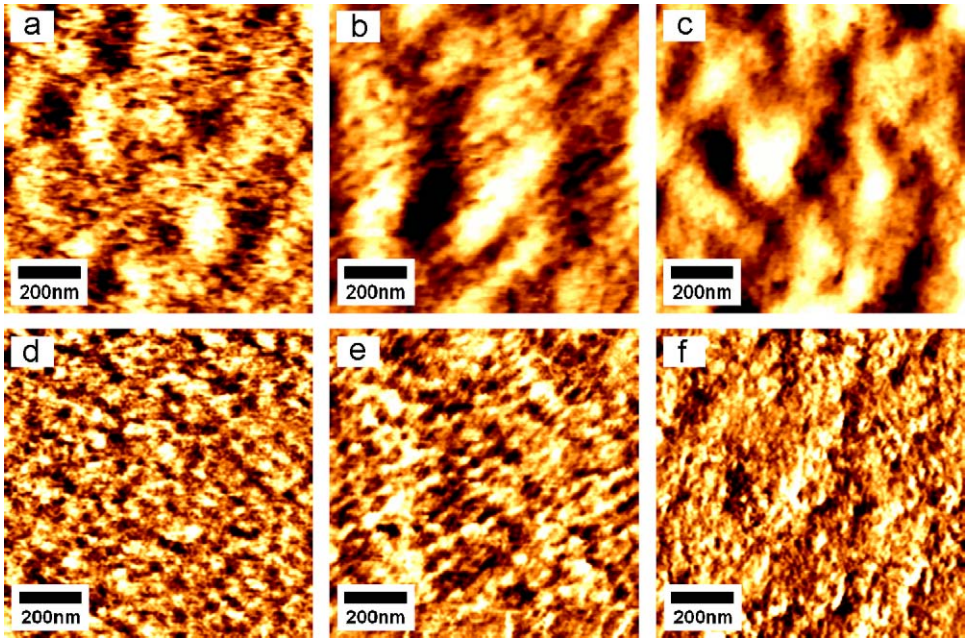

Fig. 4. Tapping mode AFM topography (top) and phase images (bottom) with different concentrations (a,d) 1 wt%, (b,e) 2 wt% and (c,f) 3 wt% of P3HT:PCBM.

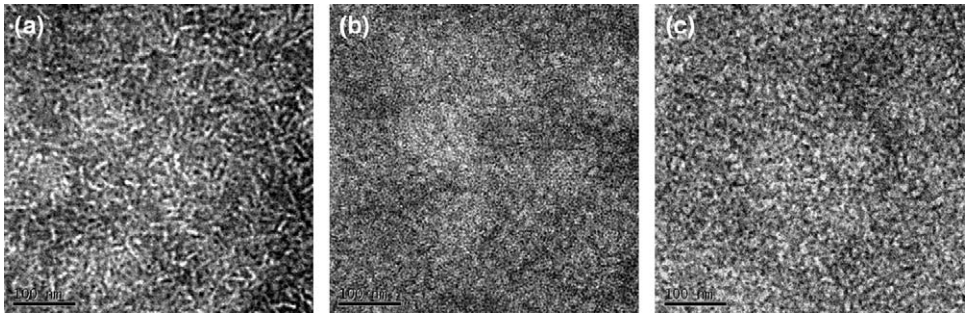

Fig. 5. FE-TEM images with different concentrations of P3HT:PCBM; (a) 1 wt%, (b) 2 wt% and (c) 3 wt%.

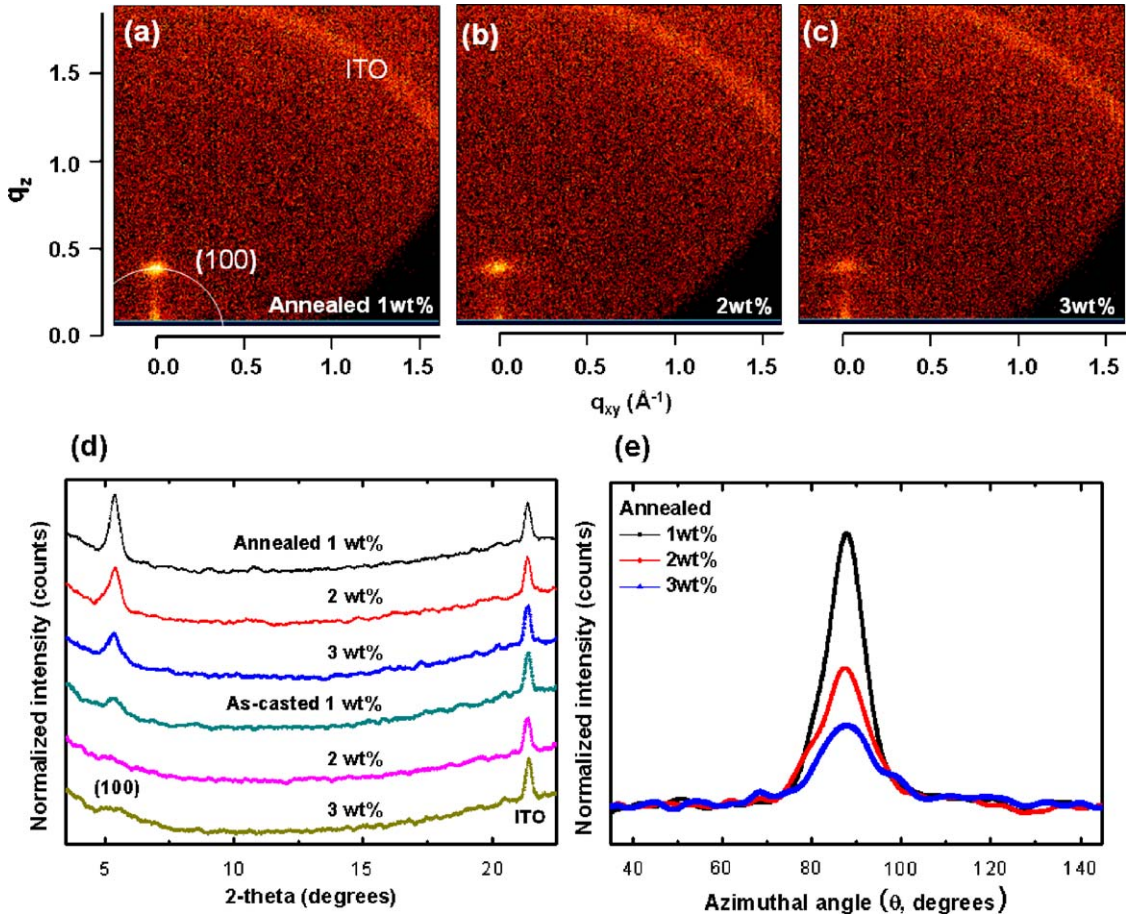

Fig. 6. 2D GIXRD patterns with different concentrations of P3HT:PCBM: (a) 1 wt%, (b) 2 wt% and (c) 3 wt%. 1D out-of-plane (d) X-ray and (e) azimuthal angle scan profiles at (1 0 0).

donor–acceptor domains with feature size of ~10 nm were observed, while fibrillar structure was only observed with 1 wt% device. It indicates that slow evaporation of solvent with low concentration of P3HT:PCBM leads to higher degree of polymer ordering which is efficient for carrier generation and transportation.

2D GIXRD patterns in Fig. 6 strongly support the results mentioned above. The peak intensity of P3HT (1 0 0) is highest for 1 wt% P3HT:PCBM device (Fig. 6(a)), and it gradually decreases for (b) 2 wt% and (c) 3 wt% devices as concentration of P3HT:PCBM is increased. Out-of-plane X-ray Fig. 6(d) and azimuthal angle scan profiles Fig. 6(e) were extracted from 2D GIXRD data (2D GIXRD data of the as-casted device not shown here). It again verifies that the crystallinity of P3HT improved by decrease in concentration of P3HT:PCBM due to slow evaporation of the solvent. Moreover, intensity of 1 wt% devices was higher than those of 2 wt% or 3 wt% device even in the as-casted devices for UV/vis spectra (Fig. 2) and XRD pattern (Fig. 6) and then indicates that even though thermal annealing is dominant factor for crystalline formation, initial drying condition of solvent during spin coating also affects the crystalline structure of polymer. As we observed certainly ordered structure of polymer by slow evaporation of solvent before thermal annealing, highly crystallized polymer was also obtained after annealing. In azimuthal scan profile, diffraction intensity with similar width is found which means that the amount of polymer molecules ordered in the same direction increased by slow evaporation of solvent with low concentration of P3HT:PCBM. Through the XRD analysis, we demonstrated crystalline polymer structure and well-ordered polymer chains by slow evaporation of the solvent with low concentration of P3HT:PCBM in the solvent.

4. Conclusion

In this paper, we report on how crystallization, interchain interaction and phase separation properties of active layer depend on concentration of P3HT:PCBM in chlorobenzene solvent. Slower evaporation of solvent with lower concentration of P3HT:PCBM leads to better crystallization, stronger interchain interaction and more ordered phase separation of P3HT not only after thermal annealing but also in the as-casted condition. With 1 wt% of P3HT:PCBM, we obtained 7.25 mA/cm^2 of J_{sc}, 0.6 V of V_{oc}, 49% of FF and 2.11% of power conversion efficiency.

Acknowledgment

This work was supported by Grant no. (ROA-2006-000-10274-0) from the National Research Laboratory Program of the Korea Science & Engineering Foundation.

References

[1] S.A. Gevorgyan, F.C. Krebs, Bulk heterojunctions based on native polythiophene, Chem. Mater. 20 (2008) 4386–4390.
[2] F.C. Krebs, H. Spanggaard, Significant improvement of polymer solar cell stability, Chem. Mater. 17 (2005) 5235–5237.

[3] J.A. Hauch, P. Schilinsky, S.A. Choulis, R. Childers, M. Biele, C.J. Brabec, Flexible organic P3HT:PCBM bulk-heterojunction modules with more than 1 year outdoor lifetime, Sol. Energy Mater. Sol. Cells 92 (2008) 727–731.
[4] X. Yang, J. Loos, S.C. Veenstra, W.J.H. Verhees, M.M. Wienk, J.M. Kroon, M.A.J. Michels, R.A.J. Janssen, Nanoscale morphology of high-performance polymer solar cells, Nano Lett. 5 (2005) 579–583.
[5] E.A. Katz, S. Gevorgyan, M.S. Orynbayev, F.C. Krebs, Out-door testing and long-term stability of plastic solar cells, Eur. Phys. J. Appl. Phys. 36 (2006) 307–311.
[6] F.C. Krebs, K. Norrman, Analysis of the failure mechanism for a stable organic photovoltaic during 10,000 h of testing, Prog. Photovolt: Res. Appl. 15 (2007) 697–712.
[7] F.C. Krebs, Air stable polymer photovoltaics based on a process free from vacuum steps and fullerenes, Sol. Energy Mater. Sol. Cells 92 (2008) 715–726.
[8] F.C. Krebs, H. Spanggard, T. Kjær, M. Biancardo, J. Alstrup, Large area plastic solar cell modules, Mater. Sci. Eng. B 138 (2007) 106–111.
[9] C. Lungenschmied, G. Dennler, H. Neugebauer, S.N. Sariciftci, M. Glatthaar, T. Meyer, A. Meyer, Flexible, long-lived, large-area, organic solar cells, Sol. Energy Mater. Sol. Cells 91 (2007) 379–384.
[10] S.E. Shaheen, R. Radspinner, N. Peyghambarian, G.E. Jabbour, Fabrication of bulk heterojunction plastic solar cells by screen printing, Appl. Phys. Lett. 79 (2001) 2996–2998.
[11] F.C. Krebs, J. Alstrup, H. Spanggaard, K. Larsen, E. Kold, Production of large-area polymer solar cells by industrial silk screen printing, lifetime considerations and lamination with polyethyleneterephthalate, Sol. Energy Mater. Sol. Cells 83 (2004) 293–300.
[12] G. Dennler, C. Lungenschmied, H. Neugebauer, N.S. Sariciftci, A. Labouret, Flexible, conjugated polymer-fullerene-based bulk-heterojunction solar cells: basics, encapsulation, and integration, J. Mater. Res. 20 (2005) 3224–3233.
[13] M. Strange, D. Plackett, M. Kaasgaard, F.C. Krebs, Biodegradable polymer solar cells, Sol. Energy Mater. Sol. Cells 92 (2008) 805–813.
[14] B. Winther-Jensen, F.C. Krebs, High-conductivity large-area semi-transparent electrodes for polymer photovoltaics by silk screen printing and vapour-phase deposition, Sol. Energy Mater. Sol. Cells 90 (2006) 123–132.
[15] T. Aernouts, P. Vanlaeke, W. Geens, J. Poortmans, P. Heremans, S. Borghsa, R. Mertensa, R. Andriessenb, L. Leendersb, Printable anodes for flexible organic solar cell modules, Thin Solid Films 451–452 (2004) 22–25.
[16] J.Y. Lee, S.T. Connor, Y. Cui, P. Peumans, Solution-processed metal nanowire mesh transparent electrodes, Nano Lett. 8 (2008) 689–692.
[17] H. Hoppe, N.S. Sariciftci, Morphology of polymer/fullerene bulk heterojunction solar cells, J. Mater. Chem. 16 (2006) 45–61.
[18] E. Bundgaard, F.C. Krebs, Low band gap polymers for organic photovoltaics, Sol. Energy Mater. Sol. Cells 91 (2007) 954–985.
[19] S. Günes, H. Neugebauer, N.S. Sariciftci, Conjugated polymer-based organic solar cells, Chem. Rev. 107 (2007) 1324–1338.
[20] M. Jørgensen, K. Norrman, F.C. Krebs, Stability/degradation of polymer solar cells, Sol. Energy Mater. Sol. Cells 92 (2008) 686–714.
[21] B.C. Thompson, J.M.J. Fréchet, Polymer–fullerene composite solar cells, Angew. Chem. Int. Ed. 47 (2008) 58–77.
[22] J.Y. Kim, K. Lee, N.E. Coates, D. Moses, T. Nguyen, M. Dante, A.J. Heeger, Efficient tandem polymer solar cells fabricated by all-solution processing, Science 317 (2007) 222–225.
[23] G. Li, V. Shrotriya, Y. Yao, Y. Yang, Investigation of annealing effects and film thickness dependence of polymer solar cells based on poly(3-hexylthiophene), J. Appl. Phys. 98 (2005) 043704.
[24] M. Reyes-Reyes, K. Kim, D.L. Carroll, High-efficiency photovoltaic devices based on annealed poly(3-hexylthiophene) and 1-(3-methoxycarbonyl)-propyl-1-phenyl-(6,6)C_{61} blends, Appl. Phys. Lett. 87 (2005) 083506.
[25] W. Ma, C. Yang, X. Gong, K. Lee, A.J. Heeger, Thermally stable, efficient polymer solar cells with nanoscale control of the interpenetrating network morphology, Adv. Funct. Mater. 15 (2005) 1617–1622.
[26] F. Padinger, R.S. Rittberger, N.S. Sariciftci, Effects of postproduction treatment on plastic solar cells, Adv. Funct. Mater. 13 (2003) 85–88.
[27] W. Ma, J.Y. Kim, K. Lee, A.J. Heeger, Effect of the molecular weight of poly(3-hexylthiophene) on the morphology and performance of polymer bulk heterojunction solar cells, Macromol. Rapid. Commun. 28 (2007) 1776–1780.
[28] P. Schilinsky, U. Asawapirom, U. Scherf, M. Biele, C.J. Brabec, Influence of the molecular weight of poly(3-hexylthiophene) on the performance of bulk heterojunction solar cells, Chem. Mater. 17 (2005) 2175–2180.
[29] T. Yamanari, T. Taima, K. Hara, K. Saito, Investigation of optimum conditions for high-efficiency organic thin-film solar cells based on polymer blends, J. Photochem. Photobiol. Chem. 182 (2006) 269–272.
[30] D. Chirvase, J. Parisi, J.C. Hummelen, V. Dyakonov, Influence of nanomorphology on the photovoltaic action of polymer–fullerene composites, Nanotechnology 15 (2004) 1317–1323.
[31] Q. Wei, T. Nishizawa, K. Tajima, K. Hashimoto, Self-organized buffer layer in organic solar cells, Adv. Mater. 20 (2008) 2211–2216.
[32] D.H. Kim, Y.D. Park, Y. Jang, H. Yang, Y.H. Kim, J.I. Han, D.G. Moon, S. Park, T. Chang, C. Chang, M. Joo, C.Y. Ryu, K. Cho, Enhancement of field-effect mobility due to surface-mediated molecular ordering in regioregular polythiophene thin film transistor, Adv. Funct. Mater. 15 (2005) 77–82.
[33] L. Fumagalli, D. Natali, M. Sampietro, E. Peron, F. Perissinotti, G. Tallarida, S. Ferrari, Al_2O_3 as gate dielectric for organic transistors: charge transport phenomena in poly-(3-hexylthiophene) based devices, Org. Electron. 9 (2008) 198–208.
[34] M.T. Rispens, A. Meetsma, R. Rittberger, C.J. Brabec, N.S. Sariciftci, J.C. Hummelen, Influence of the solvent on the crystal structure of PCBM and the efficiency of MDMO-PPV 'plastic' solar cells, Chem. Commun. 17 (2003) 2116–2118.
[35] Y. Kim, S.A. Choulis, J. Nelson, D.D.C. Bradley, Device annealing effect in organic solar cells with blends of regioregular poly(3-hexylthiophene) and soluble fullerene, Appl. Phys. Lett. 86 (2005) 063502.
[36] C.Y. Kwong, A.B. Djurisic, P.C. Chui, K.W. Cheng, W.K. Chan, Influence of solvent on film morphology and device performance of the poly(3-hexylthiophene):TiO_2 nanocomposite solar cells, Chem. Phys. Lett. 384 (2004) 372–375.
[37] C.W. Chu, H. Yang, W.J. Hou, J. Huang, G. Li, Y. Yang, Control of the nanoscale crystallinity and phase separation in polymer solar cells, Appl. Phys. Lett. 92 (2008) 103306.
[38] G. Li, V. Shirotriya, J. Huang, Y. Yao, T. Moriarty, K. Emery, Y. Yang, High-efficiency solution processable polymer photovoltaic cells by self-organization of polymer blends, Nat. Mater. 4 (2005) 864–868.
[39] G. Li, Y. Yao, H. Yang, V. Shirotriya, G. Yang, Y. Yang, "Solvent annealing" effect in polymer solar cells based on poly(3-hexylthiophene) and methanofullerenes, Adv. Funct. Mater. 17 (2007) 1636–1644.
[40] K.C. Lim, C.R. Fincher Jr., A.J. Heeger, Rod-to-coil transition of conjugated polymer in solution, Phys. Rev. Lett. 50 (1983) 1934–1937.
[41] S. Hotta, S.D.D.V. Rughooputh, A.J. Heeger, Conducting polymer composites of soluble polythiophenes in polystyrene, Synth. Met. 22 (1987) 79–87.
[42] O. Inganas, W.R. Salaneck, J.E. Osterholm, J. Laakso, Thermochromic and solvatochromic effects in poly(3-hexylthiophene), Synth. Met. 22 (1988) 395–406.
[43] H. Sirringhaus, N. Tessler, R.H. Friend, Integrated optoelectronic devices based on conjugated polymers, Science 280 (1998) 1741–1744.
[44] H. Sirringhaus, P.J. Brown, R.H. Friend, M.M. Nielsen, K. Bechgaard, B.M.W. Langeveld-Voss, A.J.H. Spiering, R.A.J. Janssen, E.W. Meijer, P. Herwig, D.M. de Leeuw, Two-dimensional charge transport in self-organized, high-mobility conjugated polymers, Nature 401 (1999) 685–688.
[45] J. Cornil, D. Beljonne, J.P. Calbert, J.L. Bredas, Interchain interactions in organic π-conjugated materials: Impact on electronic structure, optical response, and charge transport, Adv. Mater. 13 (2001) 1053–1067.